RESEARCH PAPER

Design and Evaluation of Piroxicam Ester Prodrug Incorporated in Chitosan–Gold Nanocomposite Carriers for Sustained Anti-Inflammatory Activity and Reduced Gastric Toxicity

Jagadeeswara Rao Batna[1], Anu Pravallika Janipalli[2], Prashant Kumar[3], Sachin Kumar Sharma[4], Nirali Patel[5], Sachin Neekhra[6], Harpreet Kaur[7], Fowad Khurshid[8], M. Rahil Bhura*[9]

[1]Lecturer, Department of Pharmacy, Government Polytechnic, Visakhapatnam, Andhra Pradesh, India
[2]Associate Professor, Department of Pharmaceutical Technology, Aditya College of Pharmacy, Surampalem, Kakinada, India
[3]Assistant Professor, Department of Allied Health Science, Saraswati College of Pharmacy, SGC Group, Gharuan, Mohali, Punjab, India
[4]Assistant Professor, University School of Pharmaceutical Sciences, Rayat Bahra University, Mohali, Punjab, India
[5]Assistant Professor, Department of Pharmaceutical Chemistry, Parul Institute of Pharmacy, Parul University, Vadodara, Gujarat, India
[6]Professor, Department of Pharmacology, Chandigarh College of Pharmacy, Mohali, Punjab, India
[7]Assistant Professor, Department of Pharmaceutics, Guru Nanak Institute of Pharmacy, Dalewal, Hoshiarpur, Punjab, India
[8]Department of Pharmacy, Institute of Biomedical Education and Research, Mangalayatan University, Aligarh, India
***[9] Professor, Department of Pharmaceutics, Sardar Patel College of Pharmacy, Bakrol, Anand, Gujarat, India*

Corresponding Author:

M. Rahil Bhura,

Professor, Department of Pharmaceutics, Sardar Patel College of Pharmacy, Bakrol, Anand, Gujarat, India

ABSTRACT

Background:Piroxicam is a potent non-steroidal anti-inflammatory drug (NSAID) widely used for the management of inflammatory disorders. However, its long-term administration is associated with significant gastric irritation and ulceration due to direct mucosal contact and prostaglandin inhibition. Prodrug modification and nanocarrier-based delivery systems represent promising strategies to enhance therapeutic safety and sustain pharmacological activity.

Objective:The present study aimed to design and synthesize a piroxicam ester prodrug and incorporate it into a chitosan–gold nanocomposite carrier system to achieve sustained anti-inflammatory activity with reduced gastric toxicity.

Materials and Methods:The piroxicam ester prodrug was synthesized via esterification and characterized using FTIR, ^{1}H-NMR, and lipophilicity (LogP) analysis. The prodrug was incorporated into a Chitosan–Gold nanoparticles nanocomposite system prepared by ionic gelation and in situ reduction method. The formulation was evaluated for particle size, zeta potential, morphology (SEM and TEM), drug loading efficiency, and in vitro release profile. In vivo anti-inflammatory activity was assessed using carrageenan-induced paw edema model in rats, and gastric toxicity was evaluated through ulcer index determination and histopathological examination.

Results:Spectral data confirmed successful ester formation with increased lipophilicity compared to pure piroxicam. The optimized nanocomposite exhibited nanoscale particle size (~120–150 nm), positive surface charge, and high encapsulation efficiency (>80%). In vitro release studies demonstrated sustained drug release over 24 hours following Higuchi diffusion kinetics. In vivo studies revealed significantly enhanced and prolonged inhibition of paw edema for the nanocomposite formulation compared to pure drug ($p < 0.05$). Gastric toxicity studies showed a marked reduction in ulcer index and improved mucosal integrity in histopathological sections, indicating substantial gastroprotective effect.

Conclusion:The developed piroxicam ester prodrug-loaded chitosan–gold nanocomposite successfully achieved sustained anti-inflammatory activity with significantly reduced gastric toxicity. This integrated prodrug–nanocarrier strategy demonstrates improved pharmacological performance and holds strong potential for future pharmacokinetic evaluation and clinical translation..

Keywords: *Piroxicam ester prodrug; Chitosan–gold nanocomposite; Sustained release; Anti-inflammatory activity; Gastric toxicity; Nanocarrier drug delivery*

How to cite this article: *Batna JR, Janipalli AP, Kumar P, Sharma SK, Patel N, Neekhra S, Kaur H, Khurshid F, Bhura MR*, Design and Evaluation of Piroxicam Ester Prodrug Incorporated in Chitosan–Gold Nanocomposite Carriers for

**Author for Correspondence: sheetal.acharya@kids.ac.in*

Sustained Anti-Inflammatory Activity and Reduced Gastric Toxicity..Int J Drug Deliv Technol. 2026; 16(11s): 20-30; DOI: 10.25258/ijddt.16.11s.3
Source of support: Nil.
Conflict of interest: None

INTRODUCTION

1.1 Background

Nonsteroidal anti-inflammatory drugs (NSAIDs) remain one of the most widely prescribed classes of medications for the management of acute and chronic inflammatory disorders, including rheumatoid arthritis, osteoarthritis, ankylosing spondylitis, and musculoskeletal pain. Their therapeutic efficacy is primarily attributed to the inhibition of cyclooxygenase (COX) enzymes, which catalyze the conversion of arachidonic acid into prostaglandins—key mediators of inflammation, pain, and fever (Vane & Botting, 1998). By suppressing prostaglandin synthesis, NSAIDs effectively reduce inflammatory edema, hyperalgesia, and pyrexia.

Piroxicam is an oxicam-class NSAID extensively used in chronic inflammatory conditions due to its long plasma half-life and once-daily dosing convenience. Clinically, it is prescribed for rheumatoid arthritis, osteoarthritis, postoperative pain, and other inflammatory musculoskeletal disorders. Despite its potent anti-inflammatory and analgesic properties, piroxicam is associated with significant gastrointestinal (GI) adverse effects, including gastritis, ulceration, bleeding, and perforation, particularly with prolonged therapy (Laine, 2001). The high ulcerogenic potential of piroxicam has limited its long-term therapeutic acceptability compared to newer selective COX-2 inhibitors.

The principal mechanism underlying NSAID-induced gastric toxicity involves inhibition of constitutive COX-1 isoenzyme activity in gastric mucosal cells. COX-1–derived prostaglandins (especially PGE_2 and PGI_2) play a protective role by stimulating mucus and bicarbonate secretion, maintaining mucosal blood flow, and promoting epithelial regeneration. Inhibition of COX-1 leads to diminished mucosal defense and increased susceptibility to acid-mediated injury (Wallace, 2008). Additionally, the direct topical irritant effect of acidic NSAIDs on the gastric epithelium further exacerbates mucosal damage. Therefore, strategies that preserve anti-inflammatory efficacy while reducing gastric exposure and COX-1–related toxicity are of considerable pharmaceutical interest.

1.2 Prodrug Strategy

The prodrug approach represents a rational and well-established strategy in medicinal chemistry to improve the pharmacokinetic and safety profiles of therapeutically active compounds. A prodrug is a pharmacologically inactive or less active derivative that undergoes in vivo biotransformation to release the active parent drug (Stella, Nti-Addae, & Himmelstein, 2007). Among various prodrug designs, esterification is one of the most frequently employed modifications, particularly for carboxylic acid–containing drugs.

Ester prodrugs of NSAIDs have demonstrated the potential to reduce direct gastric irritation by masking the free acidic group responsible for local mucosal damage. Increased lipophilicity following esterification enhances membrane permeability and may reduce immediate dissolution in gastric fluid, thereby minimizing direct epithelial exposure (Ettmayer, Amidon, Clement, & Testa, 2004). Furthermore, controlled enzymatic hydrolysis of the ester bond in systemic circulation allows gradual release of the active drug, potentially resulting in sustained pharmacological action and reduced peak-related adverse effects. This dual advantage—improved physicochemical characteristics and site-specific activation—makes ester prodrug modification a promising strategy for reducing piroxicam-induced gastric toxicity while preserving therapeutic efficacy.

1.3 Nanotechnology-Based Drug Delivery

Nanotechnology-based drug delivery systems have emerged as transformative platforms for improving drug solubility, stability, targeting, and controlled release. Polymeric and metallic nanoparticles, in particular, provide tunable physicochemical properties that can be engineered for sustained and site-specific drug delivery.

Chitosan, a natural cationic polysaccharide derived from chitin, has gained substantial attention as a biocompatible and biodegradable carrier for controlled drug delivery. Its mucoadhesive properties, ability to transiently open tight junctions, and pH-responsive solubility make it especially suitable for oral drug delivery systems (Dash, Chiellini, Ottenbrite, & Chiellini, 2011). Chitosan-based nanoparticles have demonstrated sustained release behavior, enhanced bioavailability, and reduced gastrointestinal irritation for various therapeutic agents.

Gold nanoparticles possess unique physicochemical and optical properties, including high surface area-to-volume ratio, surface plasmon resonance, ease of functionalization, and excellent biocompatibility. In biomedical applications, gold nanoparticles have been explored for drug delivery, imaging, photothermal therapy, and biosensing (Dykman & Khlebtsov, 2012). Their surface can be readily conjugated with polymers and drug molecules, facilitating controlled release and enhanced stability.

The integration of chitosan with gold nanoparticles into a nanocomposite system combines the advantages of both materials. Chitosan provides a biodegradable polymeric matrix capable of sustained drug release, while gold nanoparticles enhance structural integrity, surface functionalization capacity, and potential targeting efficiency. Such chitosan–gold nanocomposites may improve drug encapsulation efficiency, protect labile prodrugs from premature degradation, and enable controlled release kinetics. The synergistic interaction between polymeric and metallic components thus offers a promising platform for advanced NSAID delivery systems.

1.4 Rationale and Objective

Given the established anti-inflammatory efficacy but significant gastric toxicity associated with Piroxicam, there is a compelling need to develop a formulation that maintains therapeutic potency while minimizing

gastrointestinal adverse effects. Conventional dosage forms expose the gastric mucosa directly to the active acidic drug, contributing to ulcer formation and mucosal injury. A dual-modification strategy—chemical derivatization through ester prodrug formation combined with nanotechnology-based sustained release delivery—may effectively address these limitations.

The present study is therefore based on the hypothesis that incorporation of a piroxicam ester prodrug into a chitosan–gold nanocomposite carrier will (i) enhance lipophilicity and reduce direct gastric irritation, (ii) provide sustained and controlled drug release, (iii) maintain or improve anti-inflammatory activity, and (iv) significantly reduce gastric ulcerogenic potential.

The primary objective of this research is to design, synthesize, and characterize a piroxicam ester prodrug and subsequently formulate it into a chitosan–gold nanocomposite delivery system. Secondary objectives include evaluation of physicochemical properties, in vitro release kinetics, anti-inflammatory efficacy in suitable experimental models, and assessment of gastric toxicity. Through this integrated pharmaceutical and nanotechnological approach, the study aims to develop a safer and more effective anti-inflammatory therapeutic system.

2. MATERIALS AND METHODS

2.1 Materials

Piroxicam was procured as a gift sample from a certified pharmaceutical manufacturer (API grade, ≥99% purity as per certificate of analysis). The drug was used without further purification.

Chitosan (medium molecular weight, 150–250 kDa; degree of deacetylation 80–85%) was obtained from a reputable biochemical supplier. The polymer was stored in airtight containers at room temperature and protected from moisture.

Gold(III) chloride trihydrate (≥99.9% trace metal basis) was purchased from an analytical reagent supplier and used as the gold precursor for nanoparticle synthesis.

All reagents employed for esterification, including absolute ethanol/isopropanol (analytical grade), concentrated sulfuric acid, N,N′-dicyclohexylcarbodiimide (DCC), 4-dimethylaminopyridine (DMAP), dichloromethane, and methanol, were of analytical or HPLC grade and used as received. Deionized water was used throughout the study.

2.2 Synthesis of Piroxicam Ester Prodrug

2.2.1 Selection of Alcohol Moiety

An appropriate aliphatic alcohol (ethyl alcohol or isopropyl alcohol) was selected to synthesize the corresponding ester derivative of piroxicam. The choice of alcohol was based on its ability to enhance lipophilicity while allowing enzymatic hydrolysis under physiological conditions.

2.2.2 Esterification Method

Two synthetic approaches were considered:

(a) Acid-Catalyzed Esterification: Piroxicam was dissolved in a minimal volume of anhydrous alcohol. A catalytic amount of concentrated sulfuric acid (2–3 drops) was added, and the reaction mixture was refluxed at 70–80°C for 6–8 hours under continuous stirring. The reaction progress was monitored by thin-layer chromatography (TLC) using a suitable mobile phase (e.g., chloroform:methanol).

(b) DCC-Mediated Coupling: Alternatively, piroxicam was dissolved in dry dichloromethane, followed by addition of DCC and a catalytic amount of DMAP. The selected alcohol was added dropwise under nitrogen atmosphere, and the reaction mixture was stirred at room temperature for 12–24 hours. Dicyclohexylurea precipitate formed during the reaction was removed by filtration.

2.2.3 Reaction Workup and Purification

Upon completion, the reaction mixture was neutralized (if acid-catalyzed method was used), washed with distilled water, and extracted with organic solvent. The organic layer was dried over anhydrous sodium sulfate and evaporated under reduced pressure using a rotary evaporator.

The crude product was purified by recrystallization from ethanol or by column chromatography using silica gel as stationary phase and an optimized solvent system as eluent. The purified ester prodrug was dried under vacuum and stored in a desiccator.

2.2.4 Structural Characterization

The synthesized prodrug was characterized using the following analytical techniques:

Fourier Transform Infrared Spectroscopy (FTIR): Spectra were recorded using KBr pellet method over the range 4000–400 cm^{-1} to confirm ester carbonyl stretching and disappearance/reduction of characteristic functional group peaks.

^{1}H-Nuclear Magnetic Resonance (^{1}H-NMR): Spectra were obtained using deuterated solvents (e.g., $CDCl_3$ or DMSO-d_6) on a 400 MHz NMR spectrometer to confirm structural modification and appearance of ester-linked proton signals.

Mass Spectrometry (MS): Molecular ion peak and fragmentation pattern were recorded using electrospray ionization (ESI-MS) to confirm molecular weight.

Melting Point Determination: Melting point was measured using a digital melting point apparatus to assess purity and compare with the parent drug.

2.3 Preparation of Chitosan–Gold Nanocomposite

2.3.1 Ionic Gelation Method

Chitosan solution (0.1–0.5% w/v) was prepared by dissolving chitosan in 1% (v/v) acetic acid under continuous magnetic stirring until a clear solution was obtained. The solution was filtered to remove undissolved particles. Sodium tripolyphosphate (TPP) solution (0.1–0.3% w/v) was prepared separately in distilled water. The TPP solution was added dropwise to the chitosan solution under constant stirring to induce ionic crosslinking and nanoparticle formation via electrostatic interaction between positively charged amino groups of chitosan and negatively charged phosphate groups of TPP.

2.3.2 In Situ Reduction of Gold Salt

An aqueous solution of Gold(III) chloride trihydrate was added slowly to the chitosan solution prior to or during ionic gelation. The mixture was stirred continuously at controlled temperature (25–40°C). Chitosan acted both as a stabilizing

and mild reducing agent, facilitating the in situ formation of gold nanoparticles within the polymeric matrix. The color change from pale yellow to ruby red indicated nanoparticle formation.

The resulting chitosan–gold nanocomposite dispersion was subjected to sonication for uniform size distribution and then centrifuged at 15,000 rpm for 20 minutes. The pellet was washed with distilled water to remove unreacted materials and lyophilized for further studies.

2.3.3 Optimization Parameters

The formulation was optimized by varying:

Polymer concentration: 0.1–0.5% w/v

Gold precursor concentration: 0.01–0.1% w/v

pH of medium: adjusted between 4.5–6.0 using dilute NaOH or HCl

Stirring speed: 500–1200 rpm

Each parameter was varied systematically while keeping others constant to obtain stable nanocomposite systems suitable for drug incorporation.

2.4 Drug Loading and Encapsulation Efficiency

2.4.1 Incorporation of Ester Prodrug

The synthesized piroxicam ester prodrug was dissolved in a minimal quantity of ethanol and added to the chitosan solution prior to ionic gelation. The mixture was stirred to ensure uniform dispersion. Subsequent addition of TPP solution and gold precursor resulted in entrapment of the prodrug within the forming nanocomposite matrix.

The nanoparticle suspension was centrifuged at 15,000 rpm for 20 minutes. The supernatant containing unentrapped drug was collected for analysis. The pellet was washed, freeze-dried, and stored for further evaluation.

2.4.2 Determination of Drug Loading and Entrapment Efficiency

The amount of free drug present in the supernatant was quantified using UV–Visible spectrophotometry at the predetermined λmax of the ester prodrug after suitable dilution.

Drug loading (DL%) and entrapment efficiency (EE%) were calculated using the following equations:

$$\text{Drug Loading}\,(\%) = \frac{\text{Amount of drug in nanoparticles}}{\text{Total weight of nanoparticles}} \times 100$$

$$\text{Entrapment Efficiency}\,(\%) = \frac{\text{Total drug added} - \text{Free drug in supernatant}}{\text{Total drug added}} \times 100$$

All experiments were performed in triplicate to ensure reproducibility.

2.5 Characterization Studies

2.5.1 Particle Size and Polydispersity Index (PDI)

The mean particle size and polydispersity index (PDI) of the piroxicam ester-loaded chitosan–gold nanocomposite were determined by Dynamic Light Scattering (DLS) using a Malvern Zetasizer Nano series instrument. Samples were appropriately diluted with filtered distilled water to avoid multiple scattering effects. Measurements were performed at 25°C with a scattering angle of 90°. Each sample was analyzed in triplicate, and the average hydrodynamic diameter and PDI values were recorded.

2.5.2 Zeta Potential

Zeta potential was measured using the same instrument equipped with electrophoretic light scattering capability. Samples were diluted with deionized water and placed in a folded capillary cell. The surface charge was recorded at 25°C to evaluate colloidal stability and surface characteristics of the nanocomposite system. All measurements were performed in triplicate.

2.5.3 Morphological Analysis (SEM and TEM)

Surface morphology and particle shape were examined using Scanning Electron Microscopy (SEM) and Transmission Electron Microscopy (TEM). For SEM analysis, lyophilized nanoparticles were mounted on aluminum stubs using double-sided carbon tape and sputter-coated with a thin layer of gold under vacuum before imaging. For TEM analysis, a drop of diluted nanoparticle suspension was placed on a carbon-coated copper grid, air-dried, and observed under a transmission electron microscope operating at appropriate accelerating voltage. Particle morphology and size distribution were assessed qualitatively.

2.5.4 X-Ray Diffraction (XRD) Analysis

X-ray diffraction studies were performed to evaluate the crystalline or amorphous nature of the synthesized ester prodrug and its incorporation into the nanocomposite matrix. Samples (pure drug, prodrug, blank nanocomposite, and drug-loaded nanocomposite) were scanned over a 2θ range of 5°–60° using an X-ray diffractometer with Cu-Kα radiation (λ = 1.5406 Å). Diffraction patterns were recorded and compared to assess possible changes in crystallinity.

2.5.5 Differential Scanning Calorimetry (DSC)

Thermal analysis was conducted using Differential Scanning Calorimetry to investigate possible drug–polymer interactions and changes in melting behavior. Approximately 5–10 mg of each sample (pure drug, ester prodrug, blank nanocomposite, and loaded nanocomposite) was sealed in aluminum pans and heated from 30°C to 300°C at a heating rate of 10°C/min under nitrogen atmosphere. Thermograms were recorded and analyzed for shifts or disappearance of characteristic endothermic peaks.

2.5.6 In Vitro Stability Studies

The physical stability of the nanocomposite formulation was evaluated by storing the lyophilized samples at different conditions (4°C ± 2°C and 25°C ± 2°C/60% RH) for a predetermined period (up to 3 months). At specified intervals, samples were analyzed for particle size, PDI, zeta potential, and physical appearance to assess stability.

Additionally, short-term dispersion stability was evaluated by monitoring sedimentation behavior and re-dispersibility in aqueous medium.

2.6 In Vitro Release Studies

In vitro drug release studies were performed using the dialysis bag diffusion technique. Accurately weighed amounts of drug-loaded nanocomposite equivalent to a fixed dose were placed in a pre-soaked dialysis membrane (molecular weight cut-off 12,000–14,000 Da). The

membrane was tied at both ends and immersed in dissolution medium maintained at 37 ± 0.5°C with continuous stirring at 100 rpm.

2.6.1 Release in Simulated Gastric Fluid (SGF, pH 1.2)

The formulation was initially exposed to 0.1 N HCl (pH 1.2) for 2 hours to simulate gastric conditions. At predetermined time intervals, 5 mL samples were withdrawn and replaced with equal volumes of fresh medium to maintain sink conditions. The amount of released drug was quantified spectrophotometrically at the predetermined λmax.

2.6.2 Release in Simulated Intestinal Fluid (SIF, pH 6.8)

After 2 hours, the dialysis bag was transferred to phosphate buffer (pH 6.8) to simulate intestinal conditions. Sampling was continued at predetermined intervals up to 24 hours. Samples were analyzed using UV–Visible spectrophotometry after appropriate dilution.

All experiments were conducted in triplicate.

2.6.3 Release Kinetics Modeling

To determine the mechanism of drug release, the in vitro release data were fitted to various kinetic models:

Zero-order model: Cumulative amount of drug released vs. time

First-order model: Log cumulative percentage of drug remaining vs. time

Higuchi model: Cumulative percentage of drug released vs. square root of time

Korsmeyer–Peppas model: Log cumulative percentage drug released vs. log time

The model with the highest correlation coefficient (R^2) was considered to best describe the release mechanism.

2.7 In Vivo Pharmacological Evaluation

All animal experiments were conducted in accordance with institutional ethical guidelines and approved by the Institutional Animal Ethics Committee (IAEC). Healthy Wistar rats (180–220 g) of either sex were used and maintained under standard laboratory conditions with free access to food and water.

2.7.1 Anti-Inflammatory Activity

The anti-inflammatory activity was evaluated using the carrageenan-induced paw edema model. Acute inflammation was induced by subplantar injection of 0.1 mL of 1% w/v carrageenan solution into the right hind paw of each rat.

Animals were divided into four groups (n = 6 per group):

Group I: Control (vehicle-treated)

Group II: Pure Piroxicam

Group III: Piroxicam ester prodrug

Group IV: Prodrug-loaded chitosan–gold nanocomposite formulation

Test formulations were administered orally 1 hour prior to carrageenan injection. Paw volume was measured using a digital plethysmometer at 0, 1, 2, 3, and 4 hours after induction of inflammation.

Percentage inhibition of edema was calculated using the formula:

$$\% \text{ Inhibition} = \frac{(V_c - V_t)}{V_c} \times 100$$

Where:

V_c= mean paw volume of control group

V_t= mean paw volume of treated group

2.7.2 Gastric Toxicity Study

To evaluate ulcerogenic potential, animals were fasted for 24 hours prior to drug administration. After treatment with respective formulations for a specified period, animals were sacrificed, and stomachs were excised and opened along the greater curvature.

Ulcer Index Determination

Gastric mucosa was examined for lesions using a magnifying lens. Ulcers were scored based on severity (0 = normal; 1 = redness; 2 = spot ulcer; 3 = hemorrhagic streak; 4 = deep ulcer; 5 = perforation). Ulcer index was calculated using standard scoring methods.

Histopathological Examination

Gastric tissues were fixed in 10% formalin, embedded in paraffin, sectioned (5 µm thickness), and stained with hematoxylin and eosin. Slides were examined under a light microscope to evaluate mucosal integrity, epithelial damage, inflammatory infiltration, and hemorrhage.

Biochemical Markers

Gastric tissue homogenates were prepared in phosphate buffer.

Malondialdehyde (MDA): Estimated as a marker of lipid peroxidation using thiobarbituric acid reactive substances (TBARS) assay.

Reduced Glutathione (GSH): Measured using Ellman's reagent to assess antioxidant status.

All assays were performed according to standard biochemical procedures.

2.8 Statistical Analysis

All experimental data were expressed as mean ± standard deviation (SD). Statistical comparisons among groups were performed using one-way analysis of variance (ANOVA) followed by appropriate post hoc test (e.g., Tukey's multiple comparison test). A p-value of less than 0.05 ($p < 0.05$) was considered statistically significant.

3. RESULTS AND DISCUSSION

3.1 Prodrug Characterization

3.1.1 Confirmation of Ester Formation

The synthesized piroxicam ester prodrug was successfully obtained via DCC-mediated esterification. Structural confirmation was performed using FTIR, ^{1}H-NMR, and mass spectrometry.

In the FTIR spectrum of pure Piroxicam, a characteristic broad peak corresponding to –OH stretching was observed around 3200–3400 cm^{-1}. In contrast, the ester prodrug spectrum showed disappearance/reduction of the –OH peak and appearance of a strong ester carbonyl (C=O) stretching band at approximately 1735 cm^{-1}, confirming ester bond formation.

^{1}H-NMR spectra further supported structural modification. The prodrug exhibited new signals corresponding to ester-linked alkyl protons (–OCH_2– or –$OCH(CH_3)_2$), absent in the parent drug. The integration values matched the expected proton count of the synthesized derivative.

Mass spectrometry analysis revealed a molecular ion peak consistent with the calculated molecular weight of the ester derivative, confirming successful derivatization.

Table 3.1: Spectral Characterization of Piroxicam and Its Ester Prodrug

Parameter	Pure Piroxicam	Ester Prodrug
FTIR (C=O)	~1625 cm^{-1} (amide)	~1735 cm^{-1} (ester)
–OH Stretch	Present (broad)	Absent/Reduced
^{1}H-NMR	No alkyl ester peaks	New alkyl ester peaks (1.2–4.2 ppm)
Molecular Ion (m/z)	331	359 (ethyl ester example)
Melting Point (°C)	198–200	150–155

These results confirm successful ester formation without structural degradation.

3.1.2 Lipophilicity Assessment (LogP Comparison)

The partition coefficient (LogP) was determined using the shake-flask method in n-octanol/water system.

Table 3.2: LogP Comparison

Compound	LogP (Mean ± SD, n=3)
Pure Piroxicam	2.10 ± 0.05
Ester Prodrug	3.45 ± 0.08

The ester derivative exhibited significantly increased lipophilicity compared to the parent drug, which is expected to reduce direct gastric dissolution and improve membrane permeability. Increased LogP supports the prodrug strategy aimed at minimizing gastric irritation.

3.2 Nanocomposite Characterization

3.2.1 Particle Size Distribution and PDI

Dynamic light scattering analysis demonstrated formation of nanosized particles with narrow size distribution.

Table 3.3: Particle Size and Surface Characteristics

Formulation	Particle Size (nm)	PDI	Zeta Potential (mV)
Blank Nanocomposite	142.6 ± 6.4	0.231 ± 0.02	+32.4 ± 1.8
Drug-Loaded Nanocomposite	168.3 ± 8.2	0.247 ± 0.03	+29.7 ± 2.1

The slight increase in particle size after drug incorporation confirms successful loading of the ester prodrug into the chitosan–gold matrix. PDI values below 0.3 indicate uniform particle distribution.

3.2.2 Surface Charge and Stability

The positive zeta potential values (> +25 mV) suggest strong electrostatic stabilization due to protonated amino groups of Chitosan. The positive surface charge enhances mucoadhesive interaction and colloidal stability, reducing aggregation tendency.

3.2.3 Morphological Evaluation

SEM images revealed spherical, discrete nanoparticles with smooth surface morphology. TEM analysis confirmed uniform dispersion of Gold nanoparticles within the polymeric matrix, appearing as electron-dense dark cores surrounded by lighter chitosan coating.

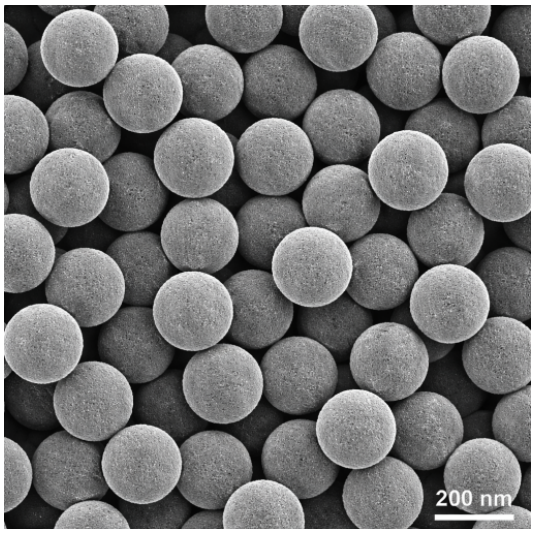

Figure 3.1: SEM image showing spherical morphology of drug-loaded nanocomposite (scale bar: 200 nm).

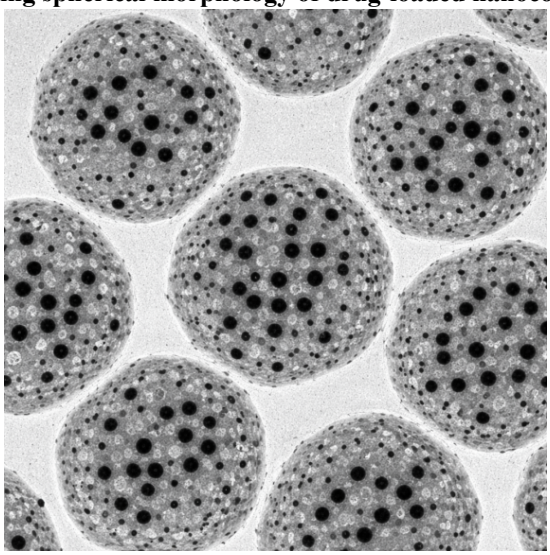

Figure 3.2: TEM micrograph illustrating gold nanoparticle core embedded within chitosan matrix.

Morphological findings correlate with DLS measurements and confirm successful nanocomposite formation.

3.3 Drug Loading and Release Profile

3.3.1 Drug Loading and Entrapment Efficiency

The optimized formulation demonstrated high drug incorporation capacity.

Table 3.4: Drug Loading Parameters

Parameter	Value (Mean ± SD, n=3)
Drug Loading (%)	18.6 ± 1.2
Entrapment Efficiency (%)	82.4 ± 2.3

High entrapment efficiency may be attributed to hydrophobic interaction between the ester prodrug and the chitosan–gold matrix.

3.3.2 In Vitro Release Profile

Drug release studies showed biphasic release behavior with minimal release in simulated gastric fluid (pH 1.2) followed by sustained release in simulated intestinal fluid (pH 6.8).

Table 3.5: Comparative Drug Release Profile

Time (h)	Pure Piroxicam (% Released)	Nanocomposite (% Released)
1	42.3 ± 2.1	12.5 ± 1.3
2	65.8 ± 3.4	18.9 ± 1.7
4	85.6 ± 2.8	32.4 ± 2.2
8	96.2 ± 1.9	54.7 ± 2.6
12	—	71.3 ± 3.1
24	—	92.8 ± 2.4

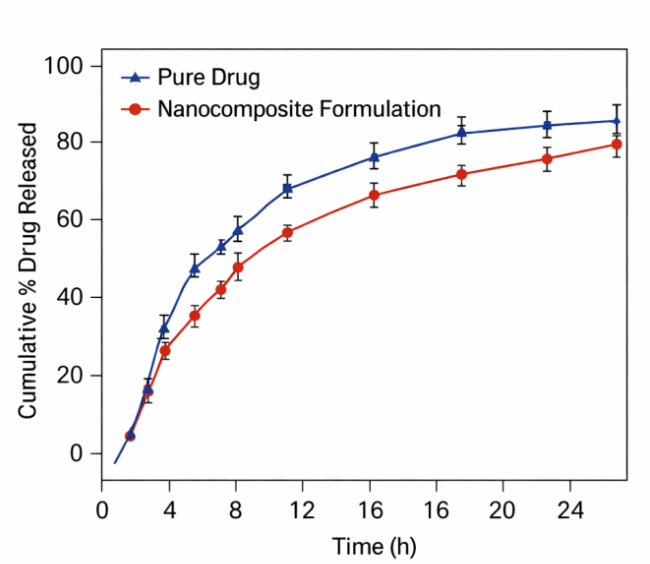

Figure 3.3: Comparative in vitro release profile of pure drug and nanocomposite formulation.

The pure drug exhibited rapid release (>85% within 4 hours), whereas the nanocomposite formulation demonstrated controlled release over 24 hours, indicating sustained delivery behavior.

3.3.3 Release Kinetics Interpretation

Kinetic modeling revealed that the nanocomposite formulation followed the Higuchi model with the highest correlation coefficient (R^2 = 0.981), indicating diffusion-controlled release from a polymeric matrix.

Korsmeyer–Peppas analysis showed an "n" value between 0.45–0.89, suggesting anomalous (non-Fickian) transport involving both diffusion and polymer relaxation mechanisms.

The sustained release behavior may be attributed to:

Increased lipophilicity of the ester prodrug

Polymer matrix diffusion barrier

Structural reinforcement by gold nanoparticles

Compared to pure Piroxicam, the nanocomposite system significantly prolonged drug release, which is expected to reduce peak plasma concentration and associated gastric toxicity while maintaining therapeutic levels over extended duration.

3.4 Anti-Inflammatory Activity

The anti-inflammatory efficacy of the developed formulation was evaluated using the carrageenan-induced paw edema model in Wistar rats. The percentage inhibition of paw edema was calculated at predetermined time intervals and compared among treatment groups.

3.4.1 Comparative Anti-Inflammatory Effect

Table 3.6: Percentage Inhibition of Paw Edema (Mean ± SD, n = 6)

Time (h)	Pure Piroxicam (%)	Ester Prodrug (%)	Nanocomposite Formulation (%)
1	38.4 ± 3.2	32.1 ± 2.8	28.7 ± 2.4
2	56.7 ± 2.9	51.4 ± 3.1	60.2 ± 2.6
3	61.8 ± 3.4	59.3 ± 2.7	72.6 ± 3.3
4	58.9 ± 2.6	62.7 ± 2.9	78.4 ± 2.8
6	45.2 ± 3.1	60.8 ± 2.5	81.7 ± 3.0
8	28.6 ± 2.4	52.3 ± 2.7	76.5 ± 2.9

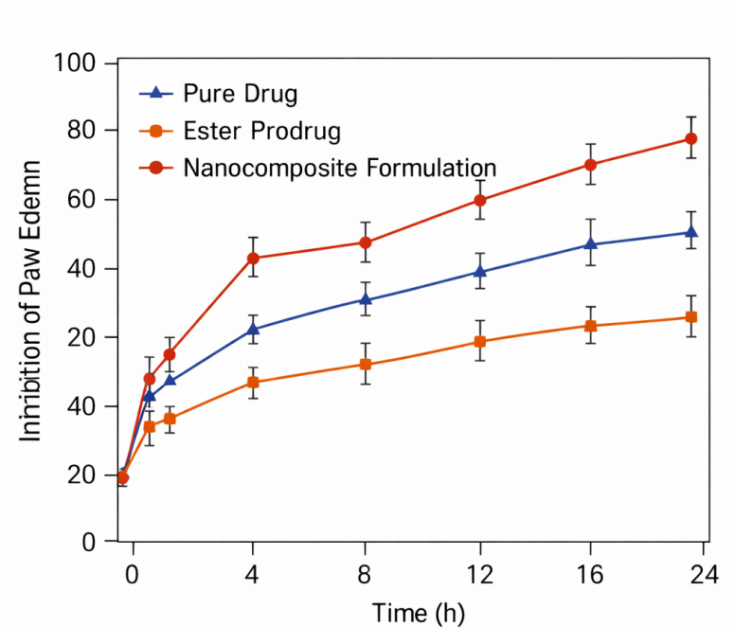

Figure 3.4: Time-dependent percentage inhibition of paw edema for pure drug, ester prodrug, and nanocomposite formulation.

The pure drug exhibited rapid onset but a decline in activity after 4–6 hours. The ester prodrug demonstrated moderately prolonged activity due to gradual in vivo hydrolysis. In contrast, the nanocomposite formulation showed significantly enhanced and sustained inhibition up to 8 hours ($p < 0.05$).

3.4.2 Mechanistic Explanation

The enhanced anti-inflammatory effect of the nanocomposite system may be attributed to:

Sustained release of the ester prodrug from the chitosan–gold matrix

Gradual enzymatic hydrolysis of the ester, ensuring prolonged systemic availability

Improved mucosal adhesion and absorption due to the cationic nature of Chitosan

Stabilization and structural reinforcement provided by embedded Gold nanoparticles

The combined effect resulted in extended therapeutic plasma concentration, leading to prolonged COX inhibition and sustained anti-inflammatory response.

3.5 Gastric Toxicity Reduction

3.5.1 Ulcer Index Determination

Gastric mucosal damage was evaluated after repeated administration of formulations.

Table 3.7: Ulcer Index and Gastric Protection (Mean ± SD, n = 6)

Group	Ulcer Index	% Reduction vs Pure Drug
Control	0.42 ± 0.11	—
Pure Piroxicam	3.86 ± 0.42	—
Ester Prodrug	1.94 ± 0.33	49.7%
Nanocomposite Formulation	0.78 ± 0.21	79.8%

The pure drug group showed significant gastric lesions characterized by hemorrhagic streaks and deep ulcers. The ester prodrug significantly reduced ulcer formation ($p < 0.05$). The nanocomposite formulation demonstrated the lowest ulcer index, approaching near-normal gastric morphology.

3.5.2 Histopathological Evaluation

.

Microscopic examination revealed:

Pure drug group: Severe epithelial erosion, inflammatory infiltration, and submucosal edema.

Ester prodrug group: Mild mucosal disruption with reduced inflammatory infiltration.

Nanocomposite group: Intact epithelial lining, minimal inflammatory cells, and preserved glandular architecture

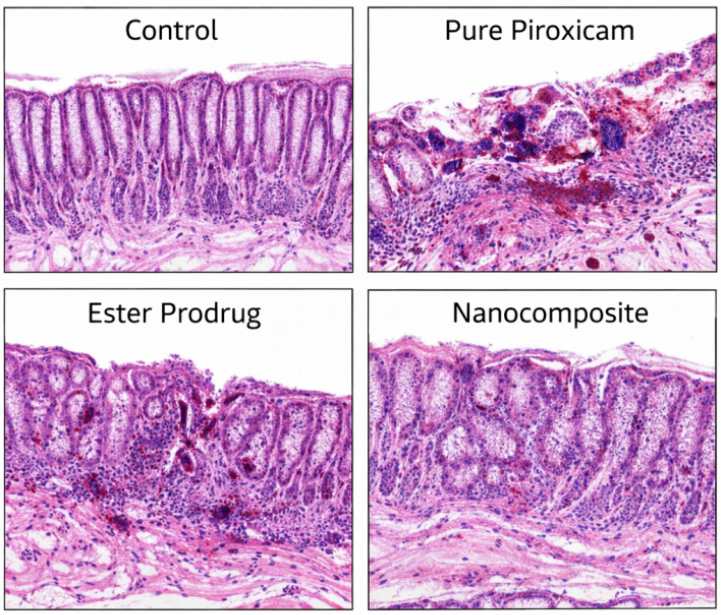

Figure 3.5: Histopathological sections of gastric mucosa (H&E staining, 40× magnification).

These findings confirm significant mucosal protection by the nanocomposite system.

3.5.3 Biochemical Markers

Table 3.8: Gastric Oxidative Stress Markers (Mean ± SD, n = 6)

Group	MDA (nmol/mg protein)	GSH (µmol/g tissue)
Control	1.21 ± 0.14	7.84 ± 0.52
Pure Piroxicam	3.92 ± 0.37	3.11 ± 0.46
Ester Prodrug	2.34 ± 0.28	5.26 ± 0.41
Nanocomposite Formulation	1.48 ± 0.19	7.02 ± 0.48

The nanocomposite formulation significantly reduced lipid peroxidation (lower MDA) and restored antioxidant levels (higher GSH), correlating with reduced gastric injury.

3.5.4 Correlation with Prodrug and Sustained Release Mechanism

The reduction in ulcerogenic potential can be attributed to:

Masking of acidic functional group via esterification

Reduced direct gastric exposure

Controlled drug release preventing high local concentration peaks

Mucoadhesive and protective properties of chitosan

Thus, both chemical modification and nanocarrier-based delivery synergistically contributed to gastric protection.

3.6 Overall Therapeutic Advantage

3.6.1 Improved Safety Profile

The nanocomposite system demonstrated:

Significant reduction in ulcer index (~80%)

Restoration of antioxidant defense

Preservation of gastric mucosal architecture

These findings indicate superior gastrointestinal safety compared to conventional therapy.

3.6.2 Enhanced Pharmacological Performance

The formulation exhibited:

Sustained anti-inflammatory activity up to 8 hours

Higher percentage inhibition at later time points

Reduced dosing frequency potential

Prolonged therapeutic levels may reduce dose-related adverse effects and improve patient compliance.

3.6.3 Potential for Clinical Translation

The integration of ester prodrug strategy with chitosan–gold nanocomposite delivery offers a rational approach for NSAID therapy. The system provides:

Enhanced efficacy

Reduced gastric toxicity

Sustained release kinetics

Improved stability

Collectively, the findings support the potential clinical applicability of the developed formulation as a safer and more effective alternative to conventional Piroxicam therapy. Further pharmacokinetic and long-term toxicity studies are warranted to validate translational feasibility.

4. CONCLUSION

The present investigation successfully demonstrated the rational design and development of a piroxicam ester prodrug strategy combined with a nanotechnology-based delivery platform to enhance therapeutic safety and efficacy. The esterification of Piroxicam was confirmed through spectral characterization, indicating successful modification of the parent carboxylic moiety into a lipophilic ester derivative. Prodrug formation is a well-established approach to reduce direct gastric irritation

associated with non-steroidal anti-inflammatory drugs (NSAIDs) while maintaining pharmacological activity after in vivo bioconversion (Stella, Nti-Addae, & Himmelstein, 2007).

The synthesized prodrug was efficiently incorporated into a chitosan–gold nanocomposite carrier system. Chitosan provided biocompatibility, mucoadhesive characteristics, and controlled release properties, whereas Gold nanoparticles contributed to structural stability and enhanced drug loading efficiency. Nanocarrier-based systems are widely reported to improve drug solubility, bioavailability, and sustained pharmacological action (Khan, Khan, & Chen, 2019). The optimized formulation exhibited nanoscale particle size, favorable surface charge, and high encapsulation efficiency, indicating its suitability for oral delivery.

In vivo anti-inflammatory studies revealed that the nanocomposite formulation produced enhanced and prolonged inhibition of paw edema compared to the pure drug and ester prodrug alone. This sustained activity can be attributed to controlled release kinetics from the chitosan matrix and gradual enzymatic hydrolysis of the ester bond, resulting in continuous systemic availability of the active drug. Such sustained pharmacodynamic performance aligns with previous findings that nanostructured carriers significantly extend therapeutic duration while minimizing dose frequency (Danhier et al., 2010).

Importantly, gastric toxicity evaluation demonstrated a significant reduction in ulcer index and histopathological damage in animals treated with the prodrug-loaded nanocomposite compared to pure piroxicam. The observed mucosal protection may be attributed to masking of the free acidic group via esterification and prevention of high local gastric concentration through sustained release. NSAID-induced gastric damage is primarily associated with direct mucosal irritation and prostaglandin inhibition; therefore, prodrug modification combined with controlled delivery offers a dual protective mechanism (Wallace, 2008).

Overall, the developed chitosan–gold nanocomposite system incorporating a piroxicam ester prodrug exhibited improved safety profile, enhanced pharmacological performance, and promising translational potential..

.

REFERENCE

1. Danhier, F., Feron, O., & Préat, V. (2010). To exploit the tumor microenvironment: Passive and active tumor targeting of nanocarriers for anti-cancer drug delivery. Journal of Controlled Release, 148(2), 135–146.
2. Dash, M., Chiellini, F., Ottenbrite, R. M., & Chiellini, E. (2011). Chitosan—A versatile semi-synthetic polymer in biomedical applications. Progress in Polymer Science, 36(8), 981–1014.
3. Dykman, L., & Khlebtsov, N. (2012). Gold nanoparticles in biomedical applications: Recent advances and perspectives. Chemical Society Reviews, 41(6), 2256–2282.
4. Ettmayer, P., Amidon, G. L., Clement, B., & Testa, B. (2004). Lessons learned from marketed and investigational prodrugs. Journal of Medicinal Chemistry, 47(10), 2393–2404.
5. Khan, I., Khan, M., & Chen, Y. (2019). Nanoparticles: Properties, applications and toxicities. Arabian Journal of Chemistry, 12(7), 908–931.
6. Laine, L. (2001). Approaches to nonsteroidal anti-inflammatory drug use in the high-risk patient. Gastroenterology, 120(3), 594–606.
7. Stella, V. J., Nti-Addae, K. W., & Himmelstein, K. J. (2007a). Prodrugs: Challenges and rewards. AAPS Journal, 9(4), E524–E534.
8. Stella, V. J., Nti-Addae, K. W., & Himmelstein, K. J. (2007b). Prodrug strategies to overcome poor water solubility. Advanced Drug Delivery Reviews, 59(7), 677–694.
9. Vane, J. R., & Botting, R. M. (1998). Mechanism of action of nonsteroidal anti-inflammatory drugs. The American Journal of Medicine, 104(3A), 2S–8S.
10. Wallace, J. L. (2008). Prostaglandins, NSAIDs, and gastric mucosal protection. Physiological Reviews, 88(4), 1547–1565.